NAVASOTA RIVER
FLOODING PROJECT

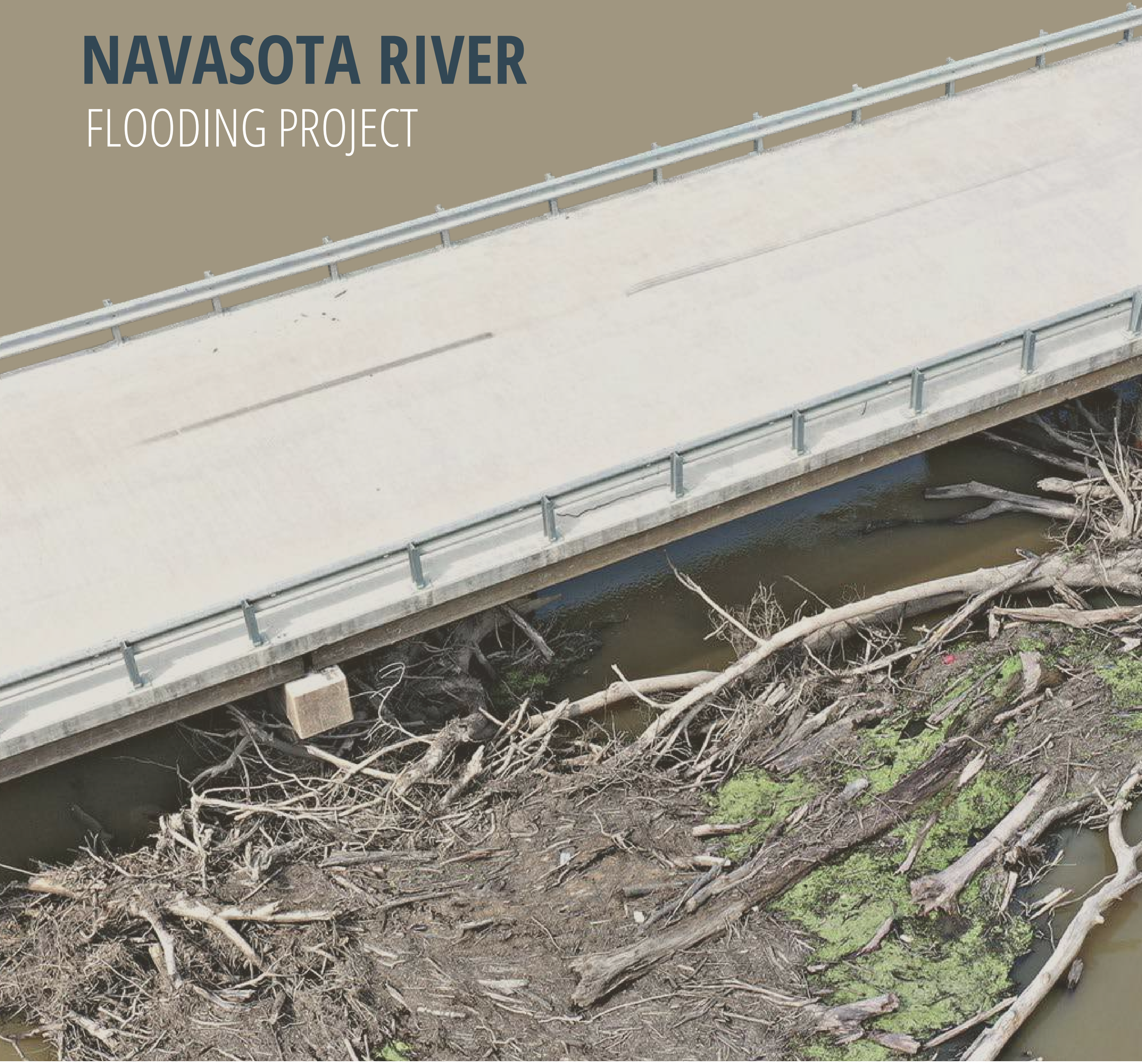

SUPPLEMENTARY MATERIALS

CHANGING ENVIRONMENTAL CONDITIONS

DECEMBER 2022

CHANGING ENVIRONMENTAL CONDITIONS

Ali Fares, Ripendra Awal, Ram Ray, Almoutaz El Hassan, Anoop Veettil, Nigus Melaku, and Atikur Rahman
College of Agriculture and Human Sciences, Prairie View A&M University

METHODOLOGICAL OVERVIEW

Data

Station precipitation data

National Centers for Environmental Information's (NCEI) Climate Data Online (CDO) provides high-quality weather data for stations covering the conterminous United States. However, the CDO precipitation data collected from the Navasota River Basin (NRB) contains many missing data. We collected rainfall data records from more than 30 stations, with missing records ranging from zero to 33 percent. Also, the collected data records ranged from short to long durations. Initially, we analyzed the accuracy of the PRISM data by comparing that data to the site-specific precipitation data through a correlation between the two data sets.

Figure 1. The Navasota River Basin (NRB) and the locations of Navarro Mills Dam (NMD) and College Station Eastwood Field (CSTN) rain gauges.

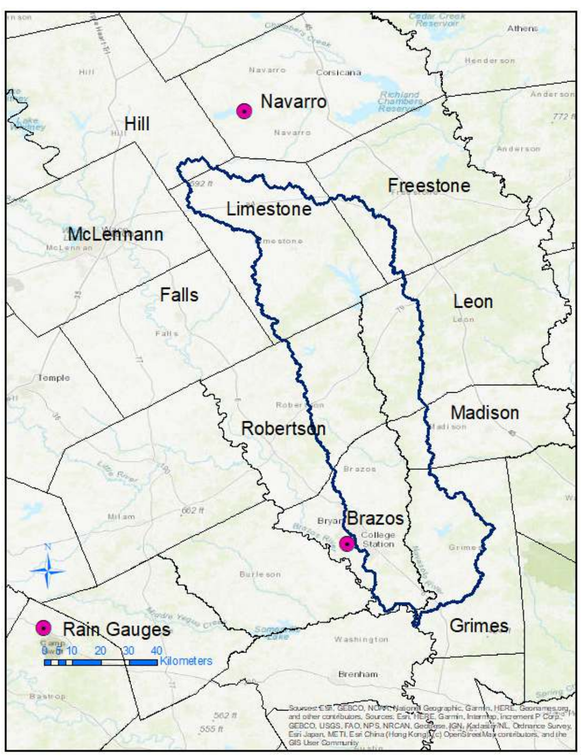

PRISM Rainfall Data

The Parameter-Elevation Regressions on Independent Slopes Model (PRISM) gridded precipitation data is available for the entire contiguous U.S. and is widely used. PRISM uses a regression analysis for about 15,000 surface precipitation measurements across the conterminous United States and produces a 4-km resolution daily precipitation product.

Streamflow Data

Data from the eight USGS streamflow gauging stations within and right below the outlet (Figure 2, Table 1) are used to evaluate the trends and change point detection. Navasota Rv Outlet is not a USGS gauging station. The approximate streamflow at the basin outlet is calculated based on the streamflow of gauging stations: Brazos Rv at Washington and Brazos Rv nr Hempstead.

Figure 2: The USGS streamflow gauging stations

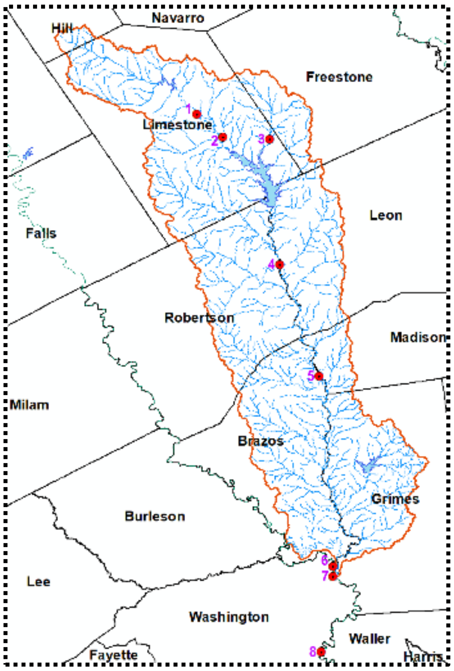

Table 1: USGS streamflow gauging stations

ID	Station Name	Duration
1	Navasota Rv abv Groesbeck	1978/06/01 - 2021/12/07
2	Navasota Rv nr Groesbeck	1965/03/01 - 1979/04/30
3	Big Ck nr Freestone	1978/07/01 - 2021/12/07
4	Navasota Rv nr Easterly	1924/03/27 - 2021/12/07
5	Navasota Rv nr Bryan	1996/10/01 - 2021/12/07
6	Brazos Rv at Washington	1965/11/01 - 1983/9/30
7	Navasota Rv Outlet	1965/11/01 - 1983/9/30
8	Brazos Rv nr Hempstead	1938/10/1 - 1987/12/31

Land Cover Data and Classes

The National Land Cover Database (NLCD) provides nationwide data on land cover and land cover change at a 30-m resolution with a 15-class legend based on a modified Anderson Level II classification system (Table 2). Among the 15 classes, sub-classes of developed, forests, wetlands, and grasslands were identified. A detailed classification up to sub- cover class level indicates accuracy level in change detection. Figure 3 shows the area coverage of each class and their change from 2001 to 2019. From the figure, it is seen that the watershed is dominantly covered by hay or pasture. A decreasing trend of hay or pastureland with time is evident from the figure.

Table 2. NLCD land cover classes in the Navasota watershed

Serial number	Object ID	Land cover class
1	12	Open Water
2	22	Developed, Open Space
3	23	Developed, Low Intensity
4	24	Developed, Medium Intensity
5	25	Developed, High Intensity
6	32	Barren Land
7	42	Deciduous Forest
8	43	Evergreen Forest
9	44	Mixed Forest
10	53	Shrub/Scrub
11	72	Herbaceous
12	82	Hay/Pasture
13	83	Cultivated Crops
14	91	Woody Wetlands
15	96	Emergent Herbaceous Wetlands

Figure 3. Area coverage of land cover classes from 2001 to 2019

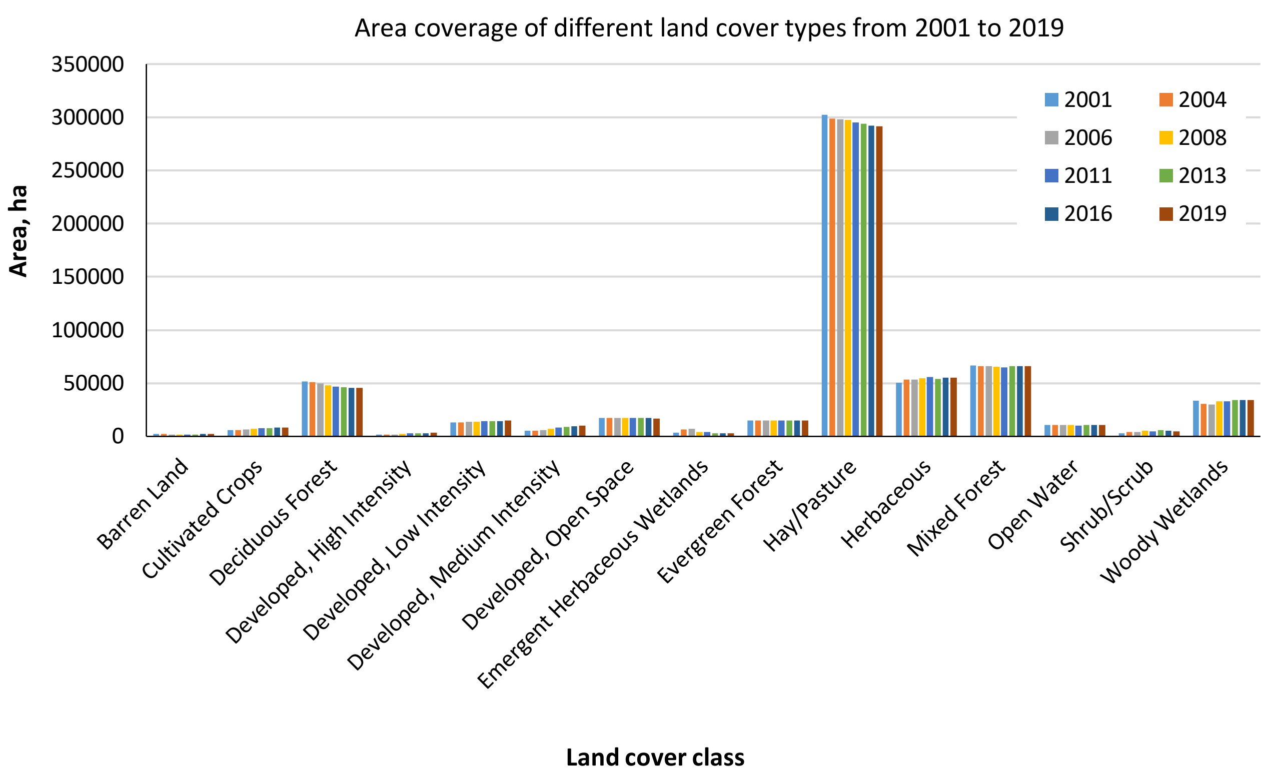

Methods

Mann-Kendall Trend Test

The nonparametric Mann-Kendall (M.K.) Trend test (Kendall, 1970) was used to analyze the precipitation and streamflow data series. M.K. test was used to identify the increasing or decreasing trends (monotonic) in Y values (e.g., precipitation). It is a nonparametric test, which means it works for all distributions, but data should have no serial correlation. A monotonic upward (downward) trend implies that the variable consistently increases (decreases) through time, but the trend may or may not be linear.

Precipitation Analysis

- Comparison of PRISM rainfall data with observed rainfall
- Spatial pattern of precipitation before and after the dam construction
- Rainfall trend analysis
- Relationship between watershed annual rainfall and average yearly flow at Navasota R.V. nr Easterly
- Rainfall: Return period analysis
- Rainfall: Change point analysis

Streamflow Analysis

The trends and change point detection at all USGS stations (Figure 2) were evaluated following the Mann-Kendall Trend Test (Kisi and Ay, 2014) and change-point analysis methods (Pettit's Test change point detection (Pettitt, 1979), respectively (Figure 4). The streamflow was evaluated to test if there is a statistically significant trend of flow during the specified period.

Figure. 4 Streamflow analysis workflow

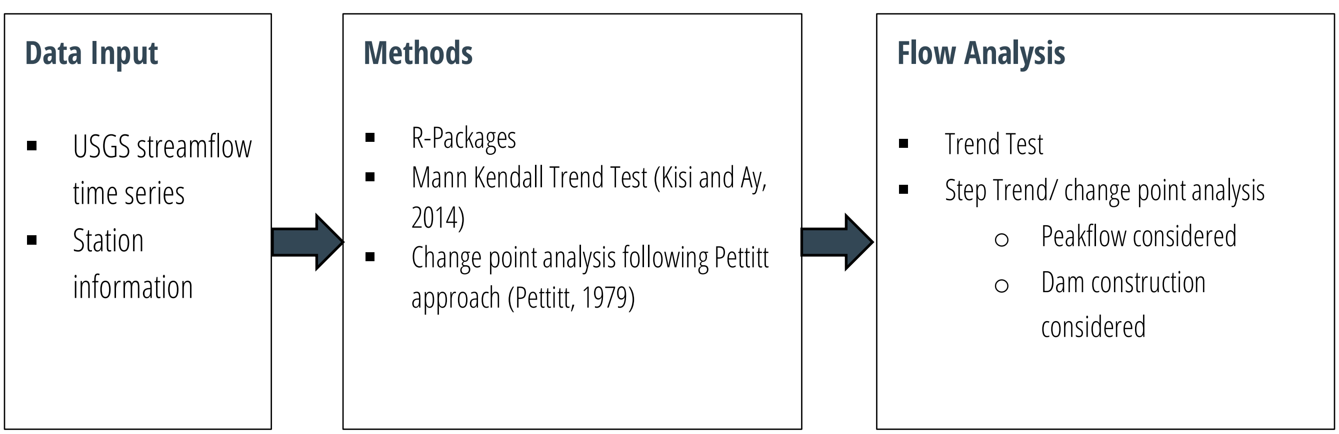

Land-Use Change Analysis

Soil and land cover characteristics and land topography are the major watershed drivers that determine the runoff-erosion timing and magnitude in response to a hydrological event in a watershed. A remarkable change in soil physical characteristics and topography is not a common phenomenon and is limited to small scales. Therefore, variation of watershed hydrologic response over time depends primarily on changes in the type and distribution of land cover. Land-use and cover change strongly impact several watershed hydrologic characteristics, including water yield, low or high flow, soil moisture, and evapotranspiration. The pronounced and direct effects of land-use and cover changes on these hydrological events have made the land-use change analysis valuable in developing catchment management policies.

Remote sensing and GIS-based methods are useful tools that have been used to quantify how much, where, and what type of land use and land cover change has occurred. Satellite imagery has been used to monitor discrete land cover types by spectral classification or to estimate biophysical characteristics of land surfaces via linear relationships with spectral reflectance or indices. Pre- and post-classification comparisons of images at spatial and temporal scales serve as the basis for change detection. In this study, classified national land cover data were used to detect land use and land cover changes. National Land Cover Database (NLCD) provides nationwide data on land cover and land cover change at a 30-m resolution with a 15-class legend based on a modified Anderson Level II classification system. The classified images were clipped into the Navasota watershed and converted to ArcGIS files format for investigating change detection. Using ArcGIS, data were analyzed through various raster and vector operations to identify and quantify spatio-temporal changes in land-use and cover types. Available land cover data from 2001 through 2019 were used in this analysis.

Hydrological Modeling

Gridded Surface Subsurface Hydrological Analysis (GSSHA) Model Overview

GSSHA is a grid-based fully-distributed parameter hydrologic model developed by the U.S. Army Corps of Engineers, Engineer Research and Development Center, Hydrologic Systems Branch. It simulates overland flow from Hortonian runoff, saturated source areas, exfiltration, and groundwater discharge to streams (Downer and Ogden, 2004). GSSHA simulates water flow after an initial calibration and validation at each grid cell for different periods. It computes hydrologic variables at each grid using several factors, including a uniform finite difference method, precipitation distribution and interception, evapotranspiration, infiltration, surface runoff routing, surface-water retention, and channel flow routing. After a specified retention depth that occurs in micro-topography, the remaining water on the land surface may runoff, causing two-dimensional overland flow.

The overland flow may eventually enter a stream and be routed to the watershed outlet as a one-dimensional channelized flow. In addition, GSSHA uses two-step explicit finite volume schemes for the diffusive wave routing method to route water for both one-dimensional channels and two-dimensional overland flow, where the flow is computed based on hydraulic heads, and volume is updated based on the computed flow using simple implicit finite difference algorithm. The diffusive wave approach allows GSSHA to route water through pits or depressions.

GSSHA can provide distributed outputs of major hydrologic variables such as soil moisture, infiltration, and runoff at high spatial and temporal resolutions. The GSSHA requires one-time calibration for an event covering all basin areas.

GSSHA Model Input

In this study, the model resolution is 500 m, and all the computations and data input were based on this resolution. GSSHA requires specific primary data processed in a particular format, including digital elevation models (DEM). The DEM data was downloaded from the National Elevation Dataset, land use from the National land Cover Dataset and soil data of the General Soil Map (STATSGO) from the National Resources Conservation Service (NRCS).

GSSHA also requires data on channel cross-sections and other properties such as channel roughness. The channel cross sections were estimated from the DEM. The cross-sections of all channels in the watershed were extracted using a Triangular Irregular Network of the DEM and river module in the GSSHA interface, Watershed Modeling System software (WMS). The raw cross-sections were edited to eliminate irregular nodes in the cross-section; that affect the flow towards the channel center. This study used the Multi-sensor Precipitation Estimator rainfall (MPE) data, available at 4×4 km and hourly resolution, which were obtained from the NWS' WGRFC online archive:
https://dipper.nws.noaa.gov/hdsb/data/nexrad/wgrfc_mpe.php). This study used NLCD land cover data for 2001 to 2019.

There are 11 USGS gauges within the Navasota River Basin. Only four gauges have a continuous streamflow measurement. Two gauges: USGS 08110800 Navasota Rv at Old San Antonio Rd near Bryan and USGS 8110500 Easterly Navasota Rv near Easterly, TX stations, are located downstream of Lake Limestone. The other two gauges are located upstream of Lake Limestone: USGS 08110325 Navasota Rv abv Groesbeck, TX (located on Navasota River downstream of Lake Mexia) and the USGS 08110430 Big Ck near Freestone, TX (located on the Big Creek a tributary of the Navasota River) (Figure 5).

Figure 5. Location of Lakes and USGS gauging stations

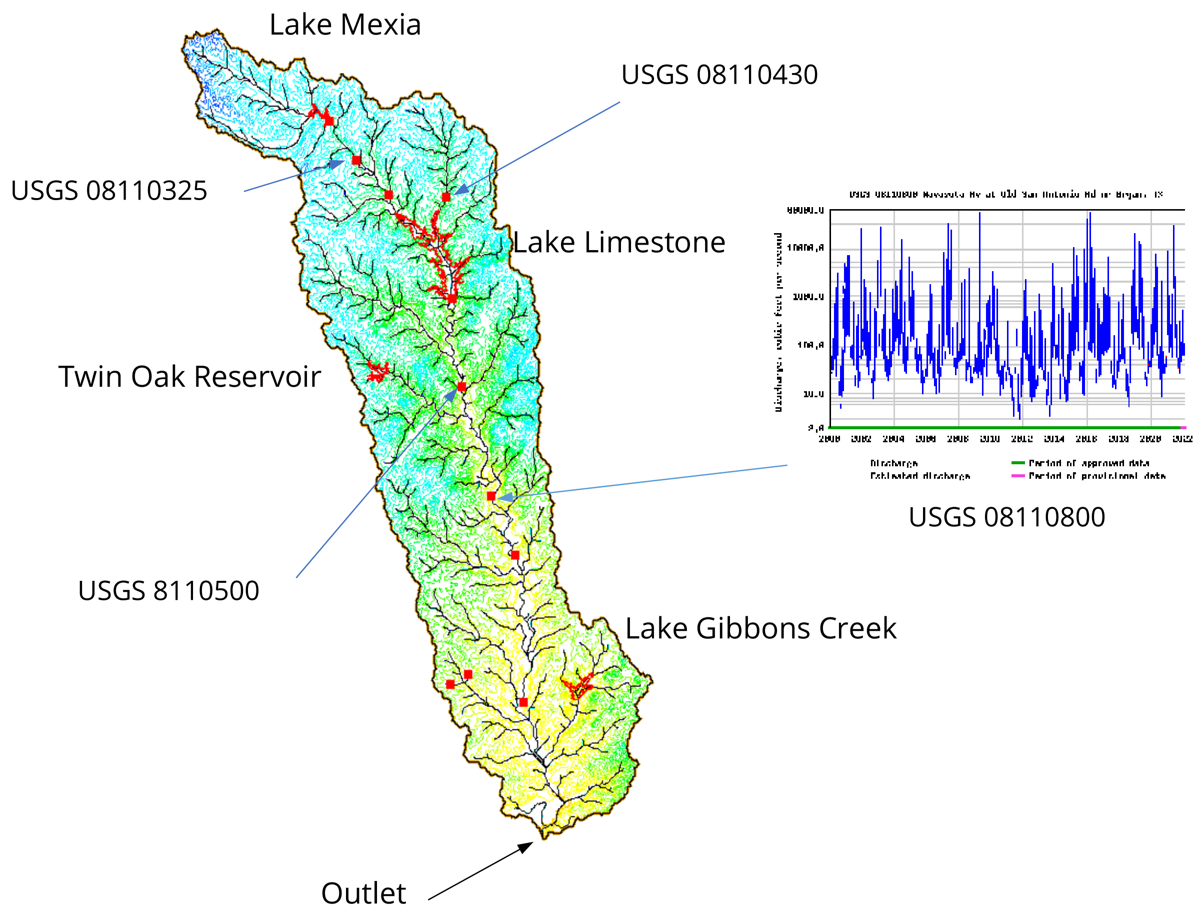

The model was calibrated and validated using selected flood events. The Stage IV Multi-Sensor Precipitation Estimator (MPE) rainfall data (4x4 km spatial and hourly temporal resolution) was used (Figure 6). MPE is a product that merges rainfall measurements from rain gauges and rainfall estimates from the NEXRAD network and the Geostationary Operational Environmental Satellite (GOES) products (Wang et al., 2008). The MPE data was downloaded for seven flooding events, and those events matched the Lake Limestone dam release data provided by BRA.

Figure 6. Multi-Sensor Precipitation Estimator (MPE) rainfall grids

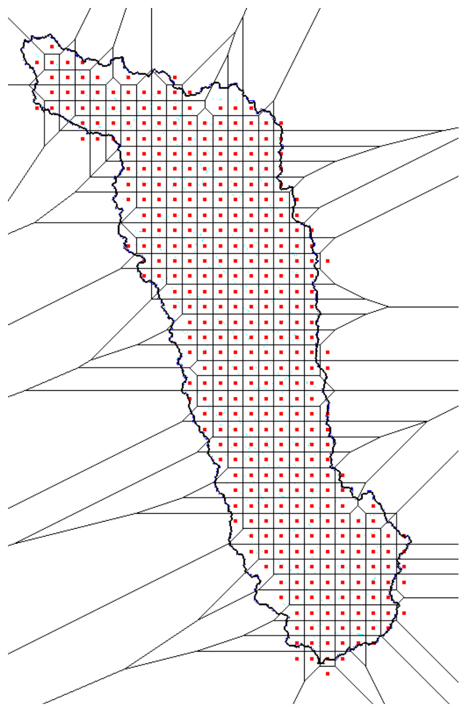

The land-use data from 2001 to 2019 were obtained from the National Land Cover Data (NLCD). Land-use data of the closest year was used in the simulation of a particular flood event. The dominant land use class in the Navasota River basin is hay/pasture and woody wetlands along the river course (Figure 7). The urban classes are concentrated in the southwest of the watershed, where the eastern part of Bryan is located. The major soil types in the basin are shown in Figure 8.

Figure 7. Land Use Data in Navasota River Basin (2006)

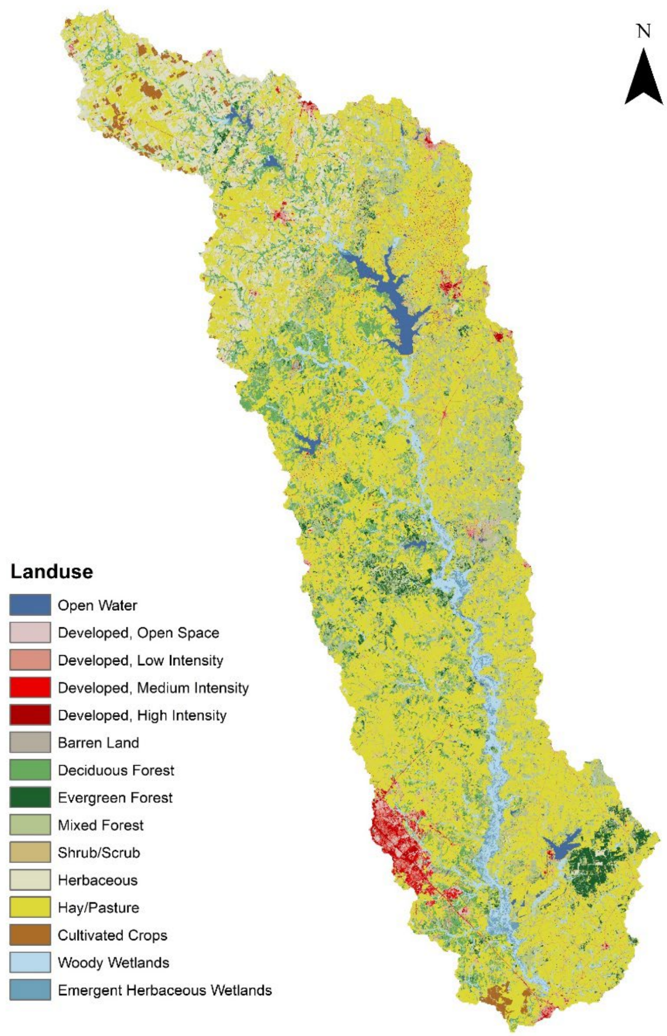

Figure 8. Soil type in Navasota River Basin

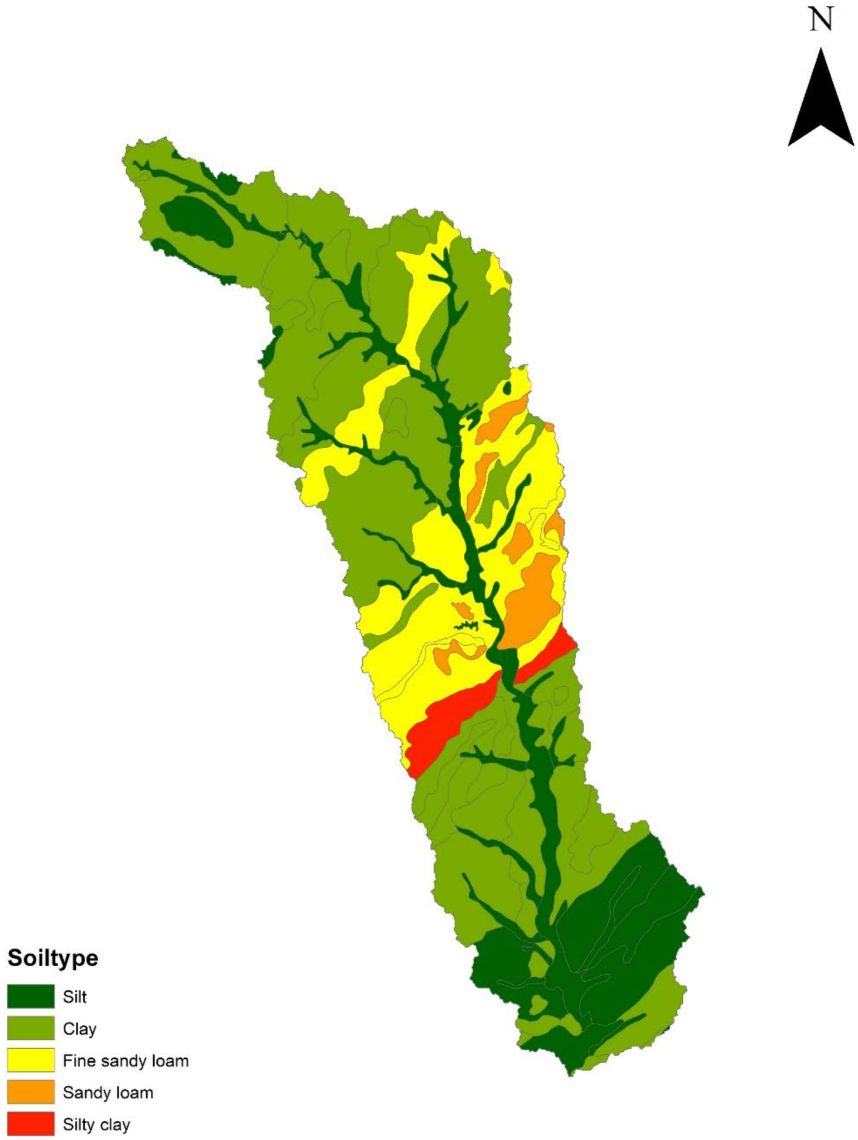

Key Findings

Precipitation

Comparison of PRISM rainfall data with observed rainfall

We analyzed the correlation between the station precipitation data and corresponding PRISM precipitation data for two gauging stations (Figure 9), with fewer missing records. The correlation (coefficient of determination, R^2) between observed and PRISM precipitation at a monthly scale is illustrated in Figure 4. For example, the station located at Navarro Mills Dam (NMD) and College Station Eastwood Field (CSTN) was 0.96 and 0.87, respectively. This indicates that PRISM and station data are highly correlated, and PRISM is acceptable for further analysis, such as seasonal precipitation trends and annual average change analyses.

Figure 9. Correlation between the monthly PRISM and observed precipitation at the gauge locations (a) Navarro Mills Dam and (b) College Station Eastwood Field.

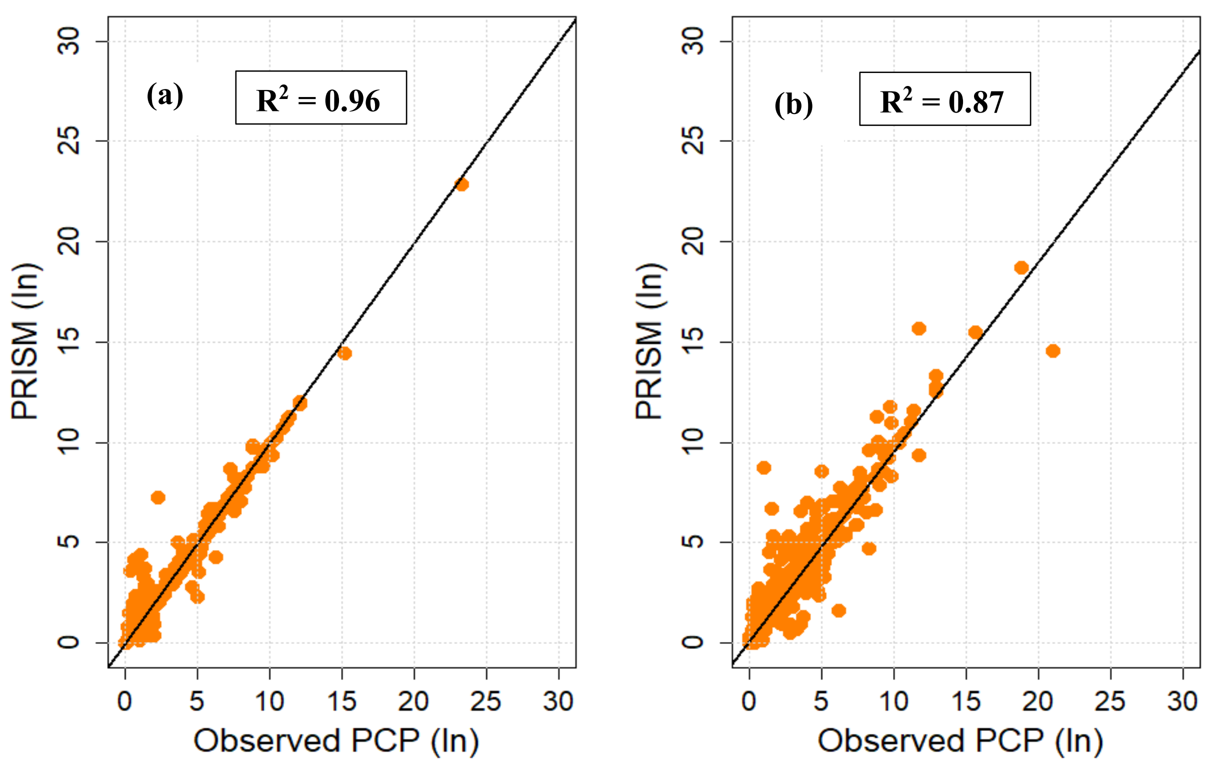

Spatial difference in precipitation pattern before and after construction of the dam

Construction of the Lake Limestone Reservoir (Sterling C. Robertson Dam) was completed in 1978, which is located about seven miles northwest of Marquez, crossing the border of Leon and Robertson Counties. To determine changes in the precipitation before and after the dam construction, we calculated the percent difference between the precipitation before (PBCD) and after (PACD) the dam construction for different time periods using the following formula: (PBCD – PACD) / (PBCD) * 100. Precipitation Before Constructing the Dam (PBCD) refers to the average annual precipitation from 1900 to 1978. For the period of the dam construction, we considered the annual average of four decades separately: 1980s (i.e., 1979 – 1988), 1990s (1989 – 1998), 2000s (1999 – 2008), 2010s (2009 – 2018), and an average of four decades (1979-2020), three decades (1989-2020), and highest rainfall year 2015. The results of this analysis are depicted in Figure 10. For example, Figure 10a, which represents the percentage change in annual average precipitation between the 1980s (i.e., 1979 to 1988) and PBCD (1900 to 1978), shows that precipitation across the basin decreased during the 1980s compared to the PBCD. Figure 10b shows that precipitation increased during the next decade (i.e., 1989 to 1998). Compared to before the dam construction period (1900 -1978), precipitation across the watershed increased by 3.7 – 14.4 % during 1979-2020, 5.1 – 18.1 % during 1989-2020, and 39 – 112 % during 2015 (Figure 11).

Figure 10. The percentage change of the PBCD (Precipitation Before Dam Construction) with the decadal precipitation after dam construction.

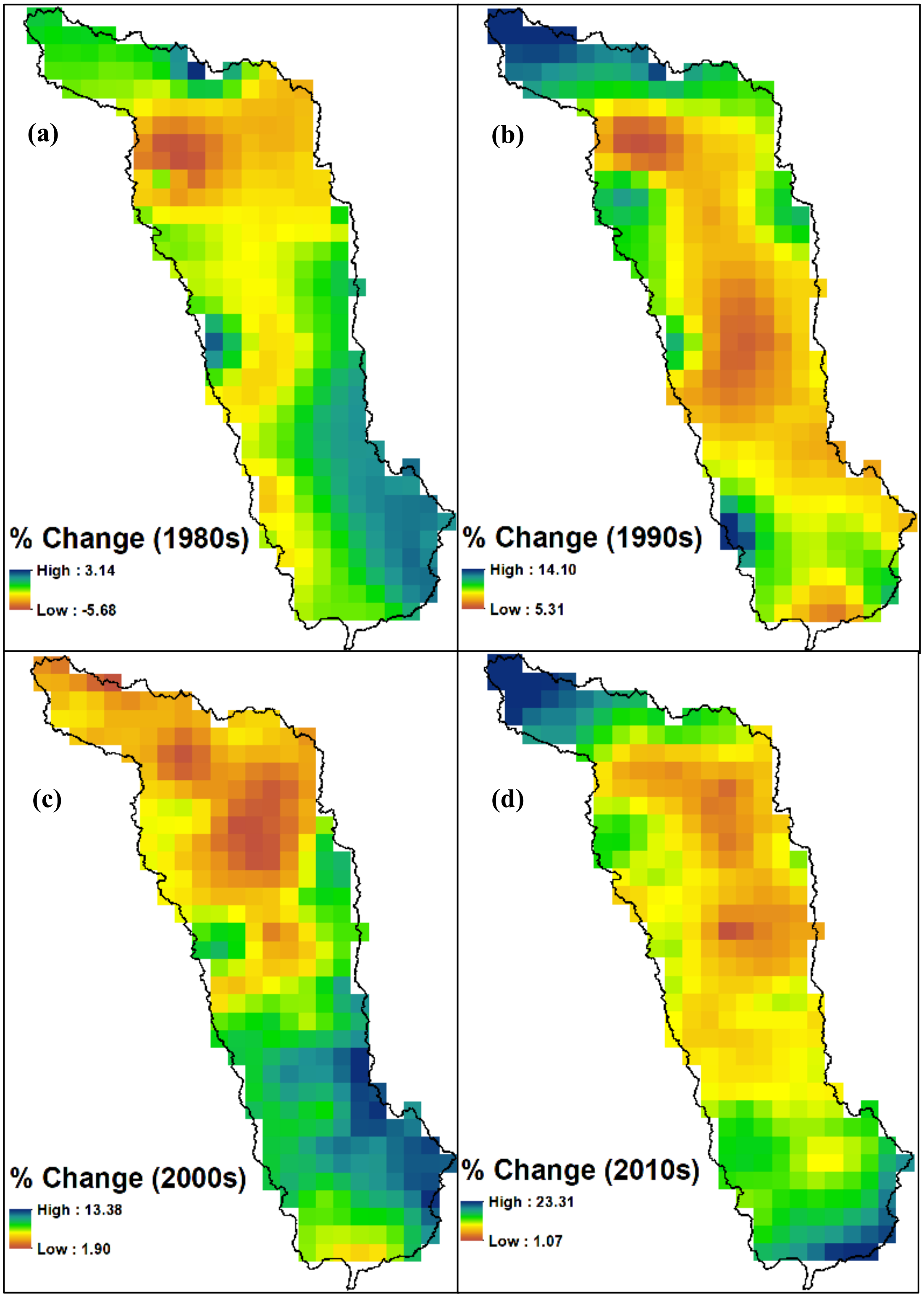

Figure 11. Spatial distribution of change in precipitation after and before constructing the dam.

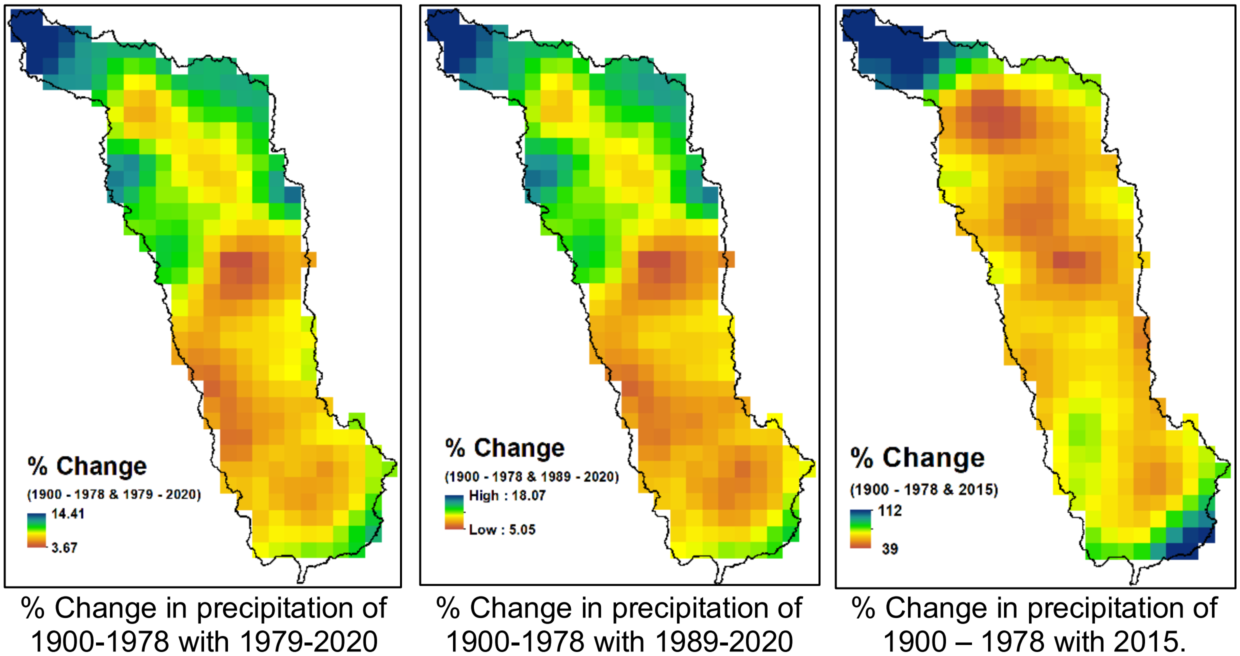

Rainfall trend analysis

A trend analysis was using a 10-year moving average precipitation in the watershed computed based on PRISM datasets, and also examined trends for each month. Watershed average decadal rolling average precipitation has a significantly increasing trend (Figure 12). The month-wise trend analysis of watershed average rainfall showed a significant monthly average watershed precipitation trend decrease in April and an increase in June (p-value <0.05) (Table 3). Here the 'tau' indicates the slope, and the positive value of tau indicates an increasing trend. Similarly, the M.K. test is performed for the station precipitation records located at NMD and CSTN.

Figure 12. Watershed average decadal rolling average precipitation trend analysis. Here tau indicates an increasing trend. The precipitation is from PRISM datasets.

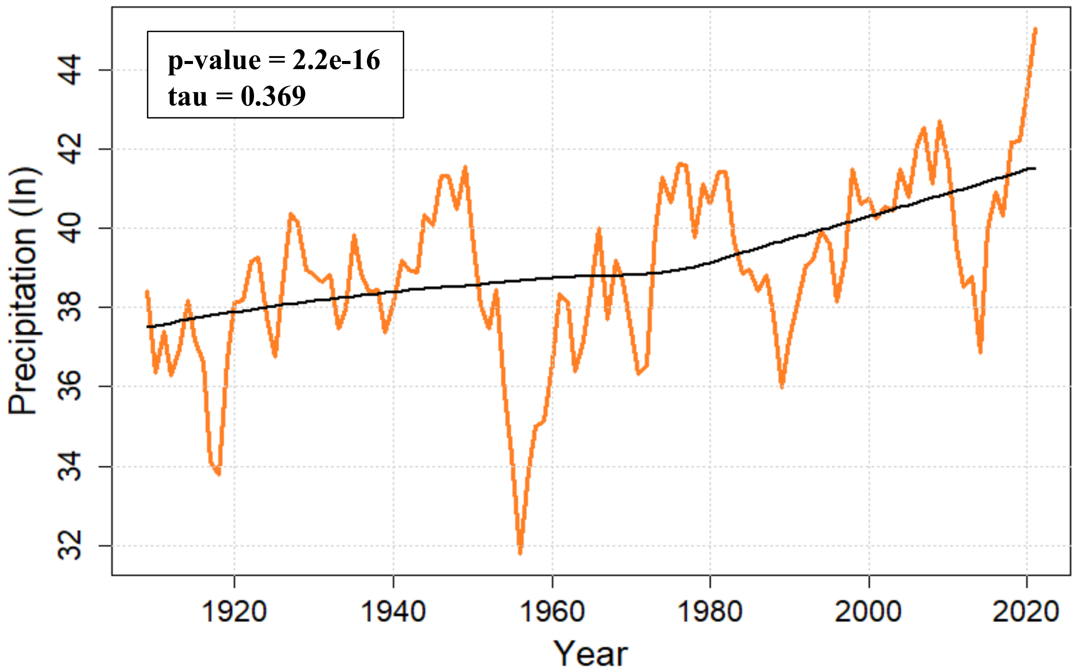

Figure 13. Watershed average monthly precipitation trend analysis. Here tau indicates a slightly increasing trend. The precipitation is from PRISM datasets.

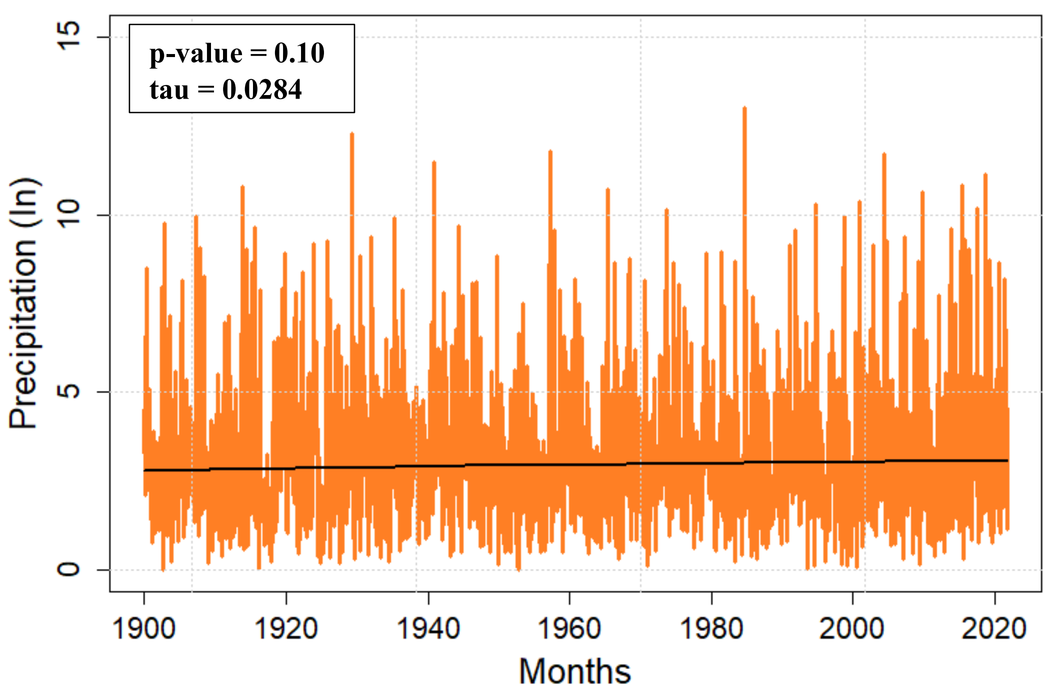

Table 3. M.K. test results for the watershed average precipitation

Month	p-value	Kendall's tau	Trend
January	0.095	0.102	
February	0.83	-0.012	
March	0.230	0.07	
April	0.04	-0.12	Significantly decreasing
May	0.067	0.025	
June	0.033	0.13	Significantly increasing
July	0.39	-0.05	
August	0.74	0.02	
September	0.23	0.07	
October	0.15	0.08	
November	0.45	0.04	
December	0.46	-0.04	

Relationship between watershed average annual precipitation and annual average flow at Navasota R.V. nr Easterly

We analyzed the correlation between the watershed averaged annual precipitation and average yearly flow at Navasota R.V. nr Easterly (Figure 14), with fewer missing records. The correlation (coefficient of determination, R^2) between precipitation and streamflow is illustrated in Figure 9.

Figure 14. Correlation between annual average flow and watershed average annual precipitation.

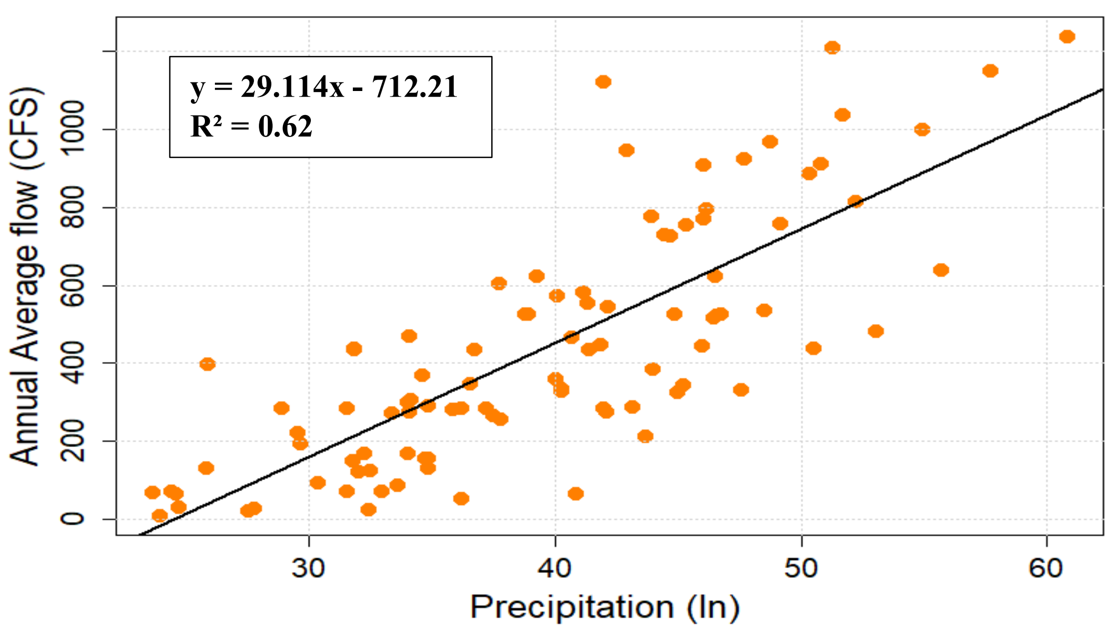

Rainfall: Return period analysis

The rainfall return periods are based on NOAA Atlas (https://hdsc.nws.noaa.gov/hdsc/pfds/). The return period for College Station Easterwood Field (CSTN) and Navarro Mills Dam (NMD) was estimated from the NOAA Atlas. The 100-year return period for CSTN (12.6 inches) was slightly higher than NMD (10.2 inches) (Figure 15).

Figure 15. Rainfall return period for (a) CSTN and (b) NMD

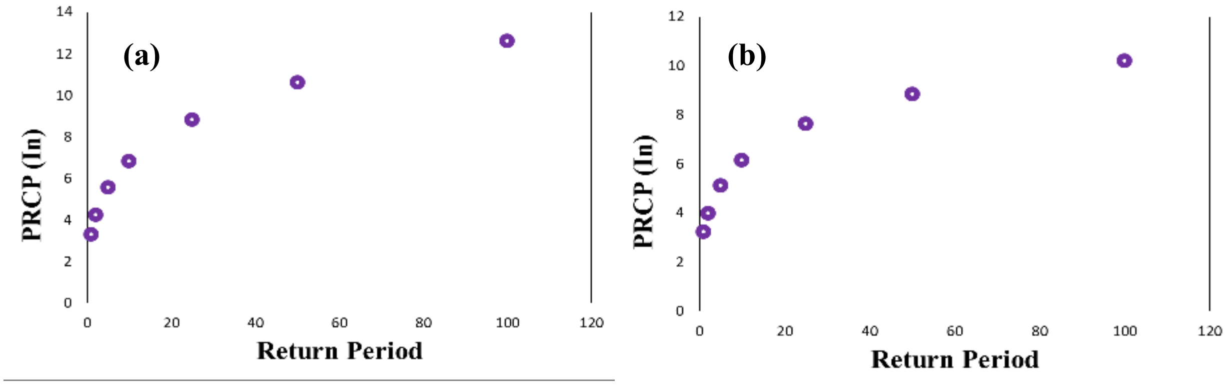

.

Rainfall: Change Point Analysis

Change point analysis detects whether any changes occurred in a rainfall time series. We applied the Pettitt test (Pettitt, 1979) for the average watershed yearly and monthly precipitation for the 1925 - 2020 period. The Pettit test quantifies the p-value of a significant change for the considered time-series input. There were no statistically significant changes detected for neither the monthly (p-value = 0.55) nor the yearly (p-value = 0.29) data.

Streamflow Trend Analysis

A 10-years moving average was calculated from the monthly peak flow series to determine long-term variations in floods. Despite the large fluctuation in the trend, the flow data reflects an apparent historical increase in the flow volume. The Mann-Kendall trend test detected statistically highly significant ($p < 0.01$) changes in the 10-years moving average trends of the monthly peak flow at the Navasota Rv nr Easterly, TX. The trend line ($p = 2.22e-16$) reflects an apparent historical increase in the higher moving monthly average downstream of lake Limestone dam (Figure 16).

Figure 16. 10-year moving average trend analysis for monthly peak streamflow at the Navasota Rv nr Easterly, TX gauge using Mann-Kendall Test.

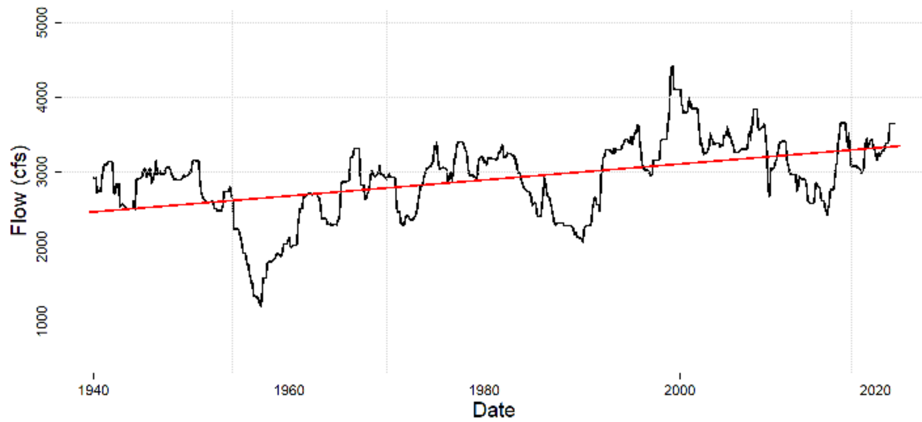

Land-Use Change Analysis

Temporal Change of Land Cover Classes

Relative to 2001, the percent change in area coverage of the different land cover classes was calculated in five-year intervals (Figure 22). The developed areas increased with time. A big jump in medium and high-intensity developments occurred during 2006 - 2011. Further analysis of the change in developed surfaces gave more detailed insights of these changes.

Figure 22. Percent change in different land cover classes at five-year intervals relative to 2001

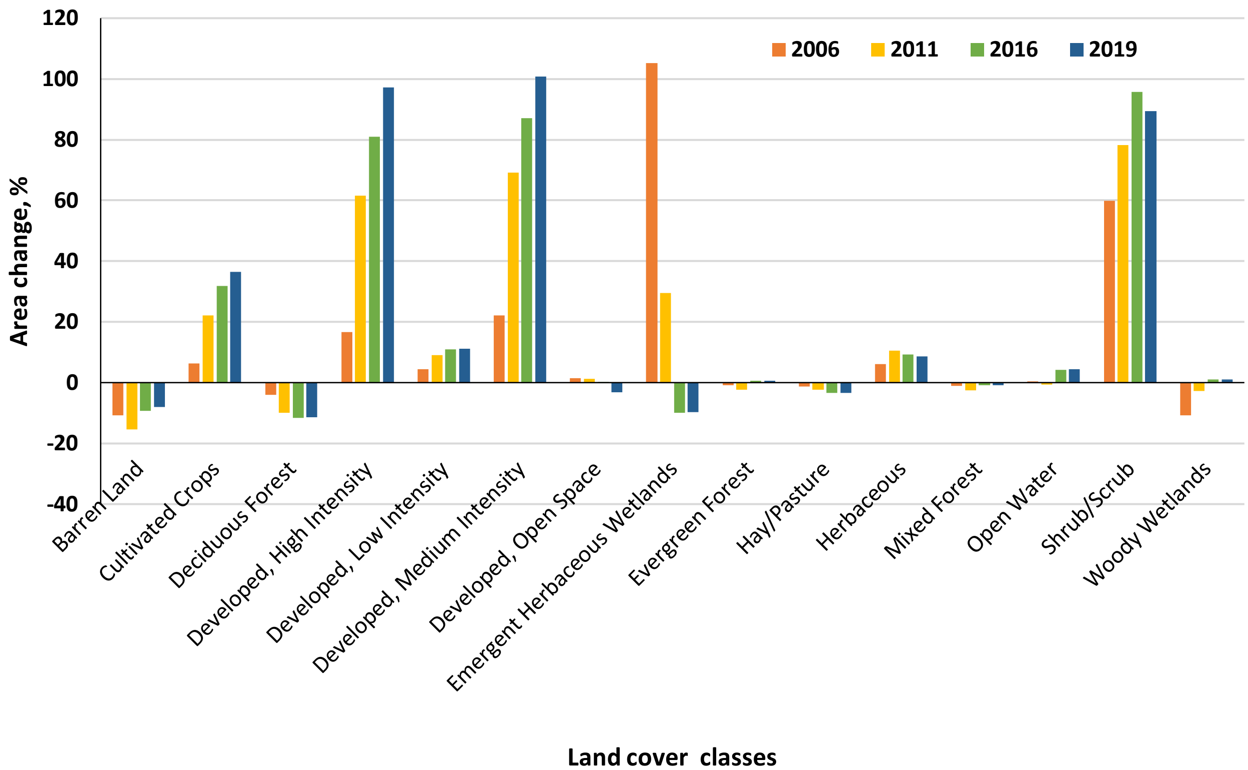

Developed Land Cover Types and Their Trend of Change

The percent change in developed surfaces of different intensities relative to 2001 at five years interval was calculated (Figure 23). A remarkable change occurred in medium and high-intensity developed surfaces.

Figure 23. Percent change in the developed surface of different intensities in five-year interval relative to 2001

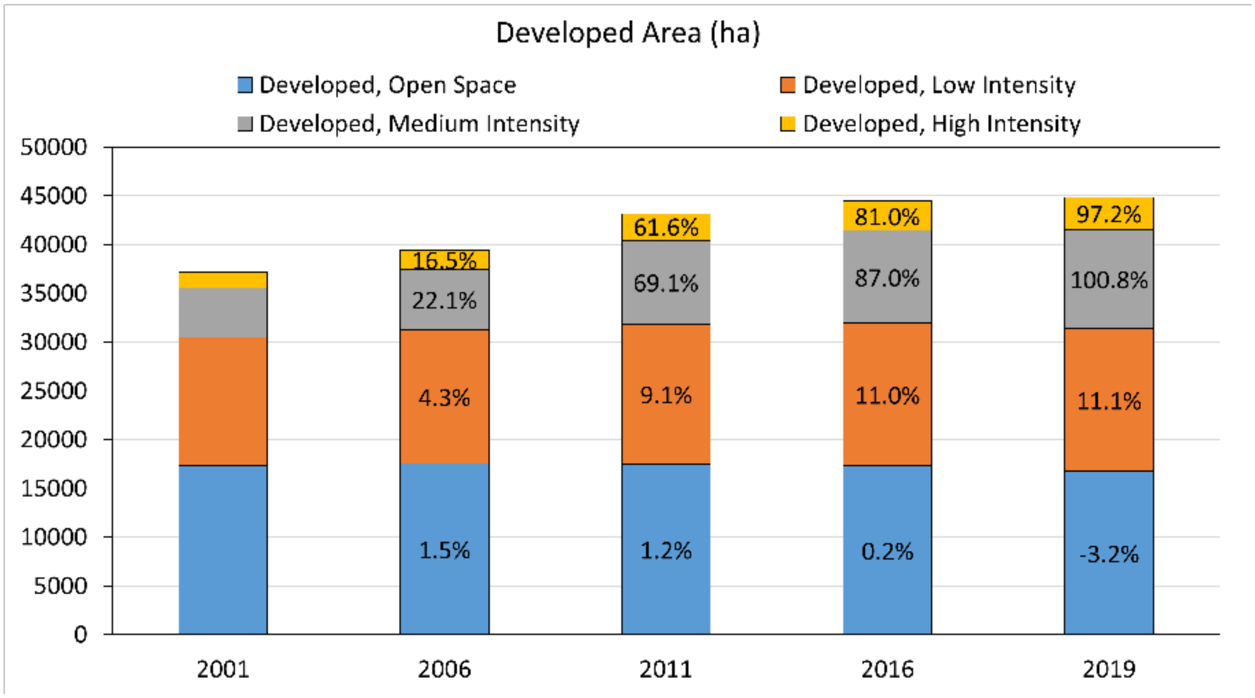

Further analysis of the change of land cover classes between 2001 and 2019 based on main classes was done (Table 4). The highest increase was observed in cultivated crops, followed by developed surfaces and open water. The overall increase in the developed surface was 20.6%. In this period, barren lands and forests decreased.

Table 4. Changes in areas of the main land cover types between 2001 and 2019

Land cover class	% Change
Barren Land	-8.08
Cultivated Crops	36.4
Developed	20.6
Forest	-4.83
Grasslands	-1.04
Open Water	4.31
Wetlands	0.03

Spatial Change in Land Cover Classes

Figure 24 shows the spatial change of land cover classes in the Navasota watershed. Visual inspection reveals that the changes are small and distributed widely throughout the watershed. However, the expansion of urban areas with more developed surfaces is evident from the figure.

Figure 24. Land-use change in the Navasota watershed between 2001 and 2019

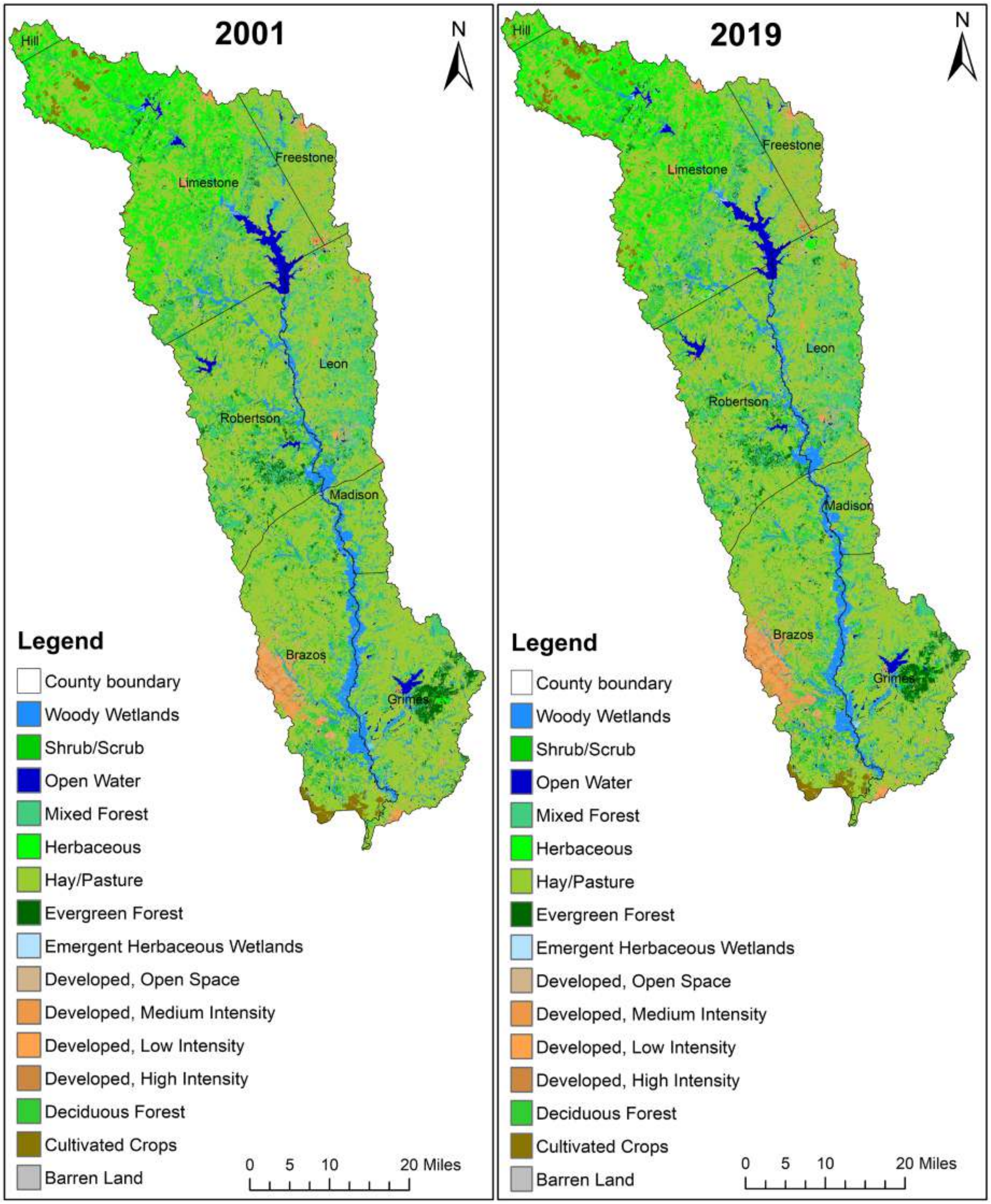

Figure 25 shows the distribution of change in the developed surface in different counties under the Navasota watershed. It is apparent that the intensity of change in developed surfaces is concentrated in urban areas.

Figure 25. Land-use change to the developed surface and its countywide distribution

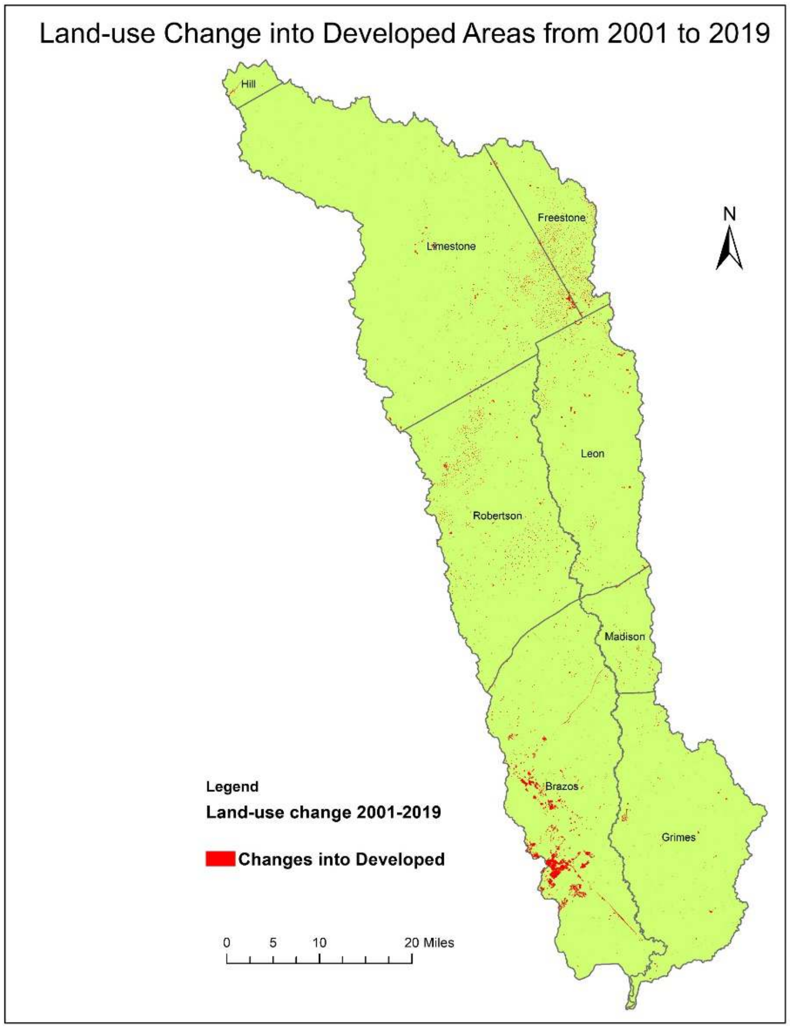

Hydrological Modeling

The Gridded Surface Subsurface Hydrological Analysis (GSSHA) was used to understand the hydrology of the watershed, simulate major previous flooding events, the effects of precipitation, and land-use changes on the flooding events and surface runoff. The model covered the entire basin.

Model calibration and validation

All calibration, validation, and scenario simulations were driven by different flooding events selected based on BRA's available dam release data. The following table shows details of the selected flood events. All comparisons between observed and simulated discharges were based on 15 minutes time interval discharge.

Table 5. Selected scenarios and flood events

S. No.	Scenarios	Flood event
1	Effect of land-use change	5/31 to 06/08/2021
2	Effect of precipitation magnitude change	5/11 to 5/20/2015

The model was calibrated for the flooding event that occurred from 12/24/2018 to 01/05/2019. This event had two flood peaks. The Dam release from Lake Limestone was also considered in the model calibration. The model was calibrated by comparing the simulated and observed discharge at four USGS gauges (Figure 5).

The first calibration stream gauge station was USGS 08110430 Big Ck nr Freestone, TX (Figure 26). Model performance measures showed that the Nash coefficient was 0.6, and the errors at the first and second peaks were 7% and 14%, respectively.

Figure 26. Comparison of simulated and observed streamflow at gauge 08110430 Big Ck nr Freestone, TX

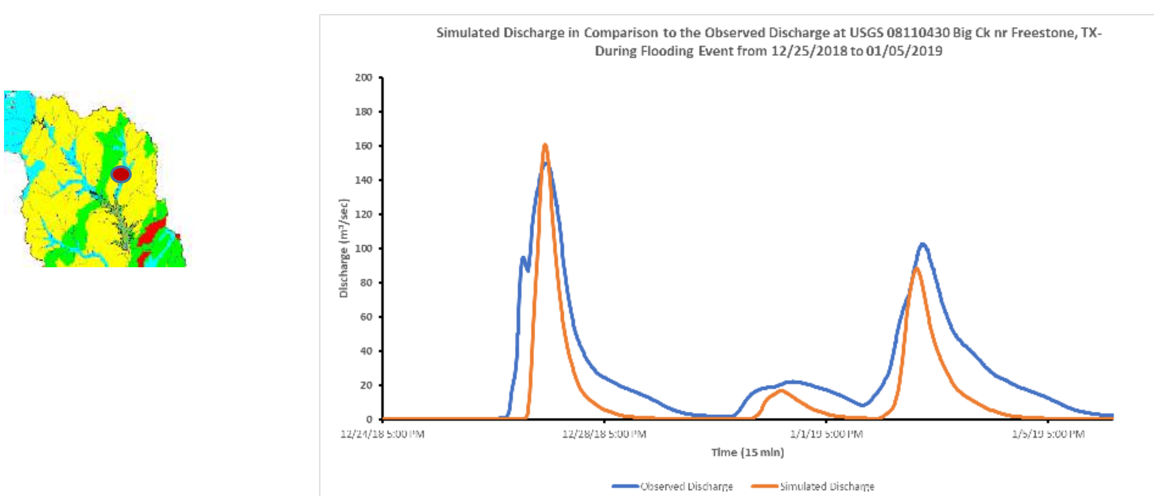

The second calibration location was USGS 08110325 Navasota Rv abv Groesbeck, TX. This gauge is located downstream of Lake Mexia, which was not simulated in this run due to the lack of Lake Mexia Dam's release data. It questions the effect's magnitude of lake Mexia on the two peaks' discharge (Figure 27). Performance measures showed that the Nash coefficient was 0.9, the error at the first peak was 21%, and 0.4% at the second peak.

Figure 27. Comparison of simulated and observed streamflow at gauge 08110325 Navasota Rv abv Groesbeck, TX

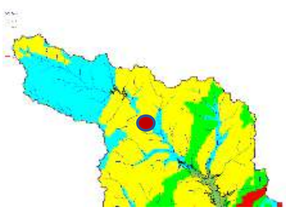

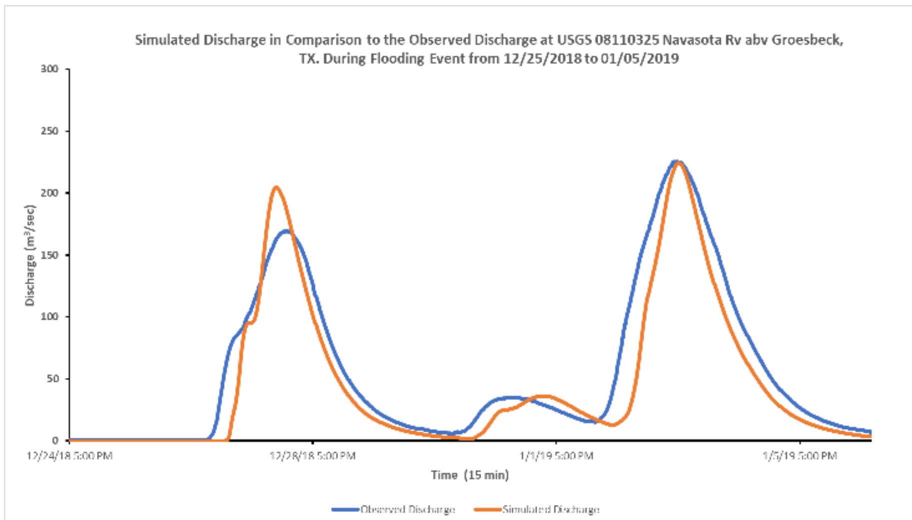

The third calibration location was downstream of Lake Limestone at USGS 08110800 Navasota Rv at Old San Antonio Rd nr Bryan, TX. Calibration's simulation includes the Dam simulation and dam release data. The performance measures showed that the Nash coefficient is 0.8, the error at the first peak was 52%, and the error at the second peak was 4%. The simulation has an overestimation at the first peak and almost matches the second peak, which is higher than the first one (Figure 28).

Figure 28. Comparison of simulated and observed streamflow at gauge 08110800 Navasota Rv at Old San Antonio Rd nr Bryan, TX

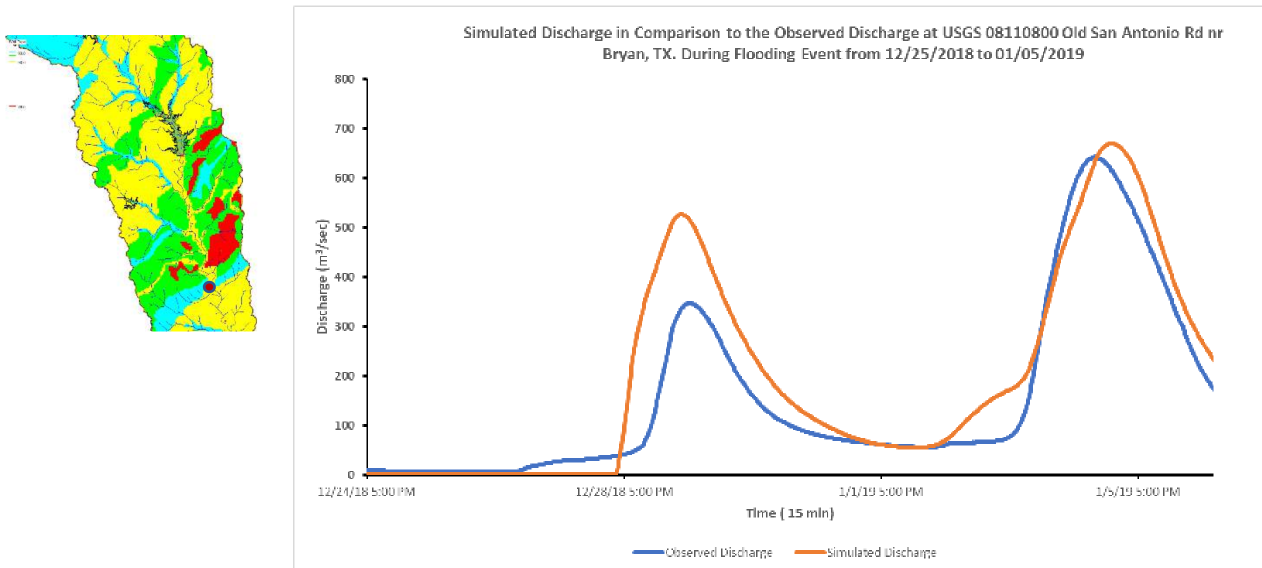

The fourth calibration location was at USGS 8110500 Easterly Navasota Rv nr Easterly, TX. The performance measures showed that the Nash coefficient was 0.7, the error at the first peak was 29%, and 18% at the second peak (Figure 29).

Figure 29. Comparison of simulated and observed streamflow at USGS 8110500 Easterly Navasota Rv nr Easterly, TX

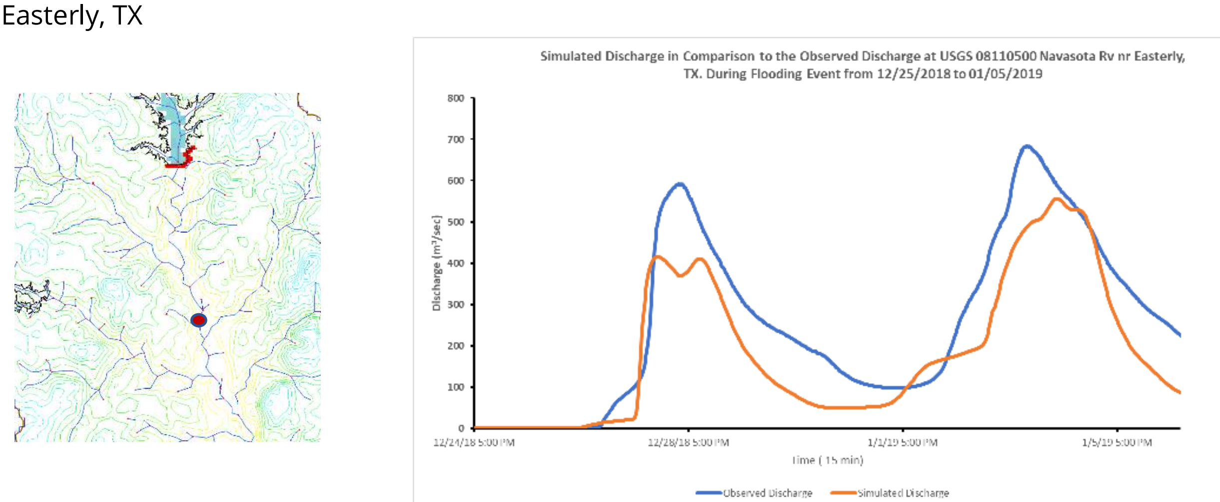

The validation event was during 05/31/2021 - 06/08/2021. The following result sowed a comparison of simulated and observed flow at USGS 08110800 Navasota Rv at Old San Antonio Rd nr Bryan, TX. This simulation also includes Lake Limestone Dam's simulation and discharge release data from BRA. Performance measures showed that the Nash coefficient was 0.9, and the error at the peak was 12% (Figure 30).

Figure 30. Comparison of simulated and observed streamflow at USGS 08110800 Navasota Rv at Old San Antonio Rd nr Bryan, TX (Validation)

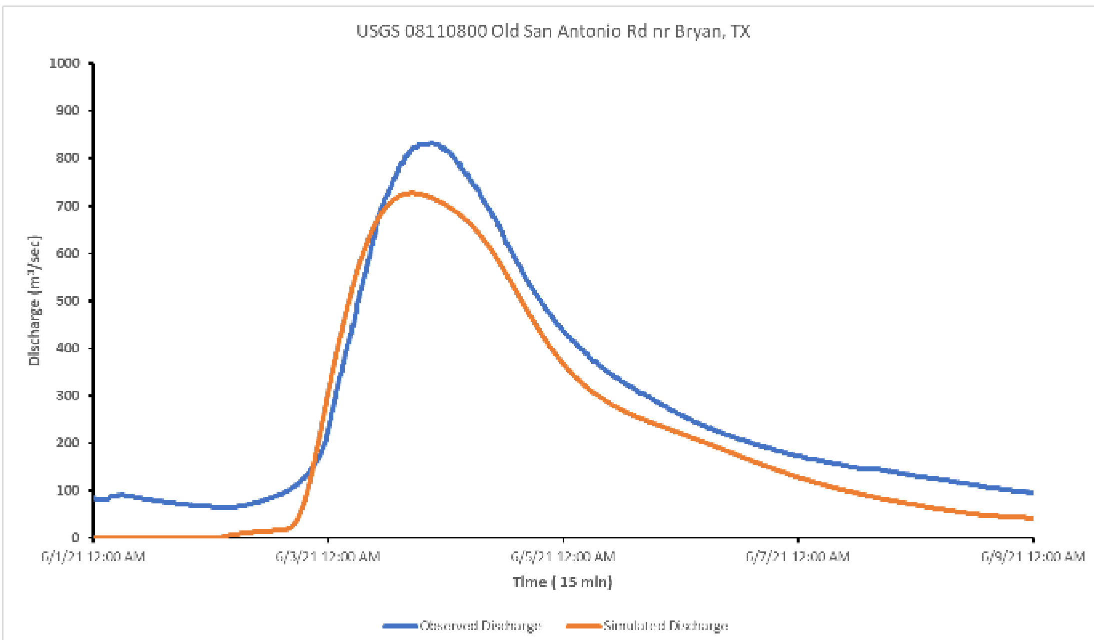

Scenario Analysis

Effect of Land-Use Change

This scenario is to evaluate the effect of land use on the discharge downstream of Lake Limestone. Two data sets of land use were implemented in the simulation. The sets were from two different surveying years. The first set was 2001 land use data and the second one was 2019 land use data. Two simulations were run for the 5/31/2021 - 06/08/2021 flood event using the 2001 and 2019 land uses. The comparison of the two simulation results revealed that land-use change as depicted in 2019 land use significantly increased runoff in urban areas (5 to 24% in some selected locations, Figure 31).

Figure 31. Comparison of streamflow at four locations with land-use of 2001 and 2019.

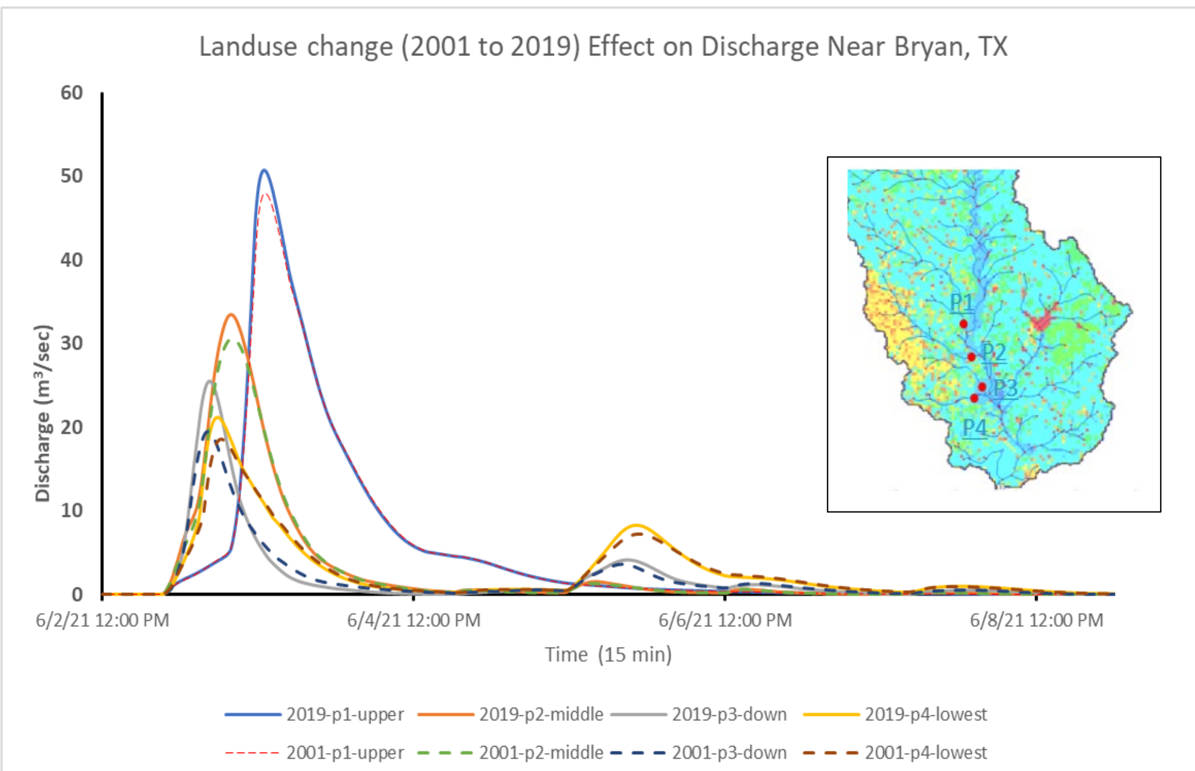

Figure 32. Location of subbasins.

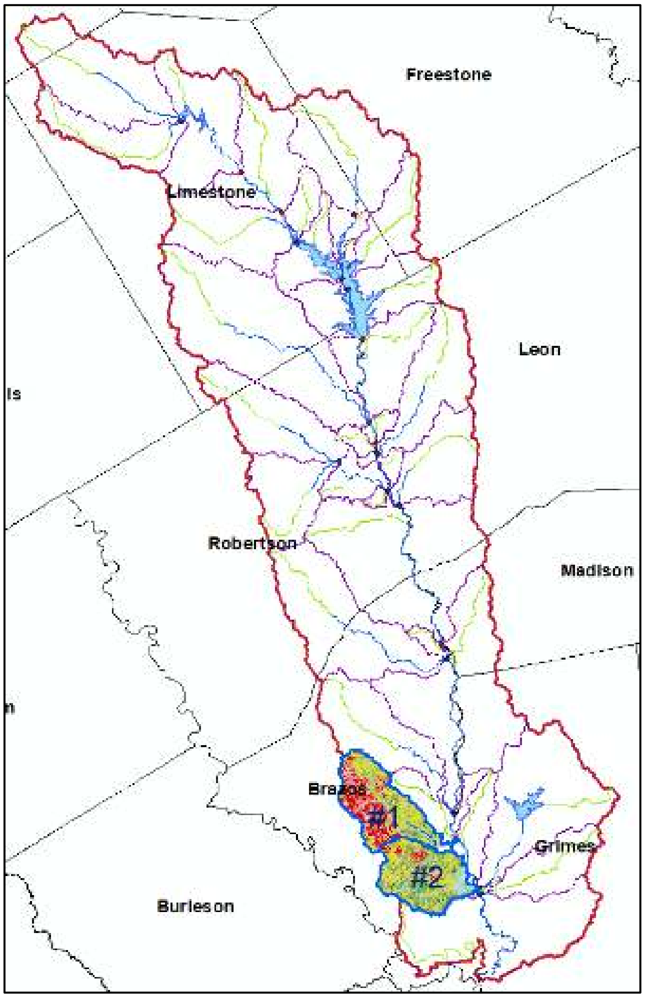

We also simulated the impact of land use on the same urban areas using the Soil & Water Assessment Tool (SWAT) model for the entire 2005-2020 period with the two land uses (2001 and 2019) (Figure 32).

Simulation results showed a substantial increase in developed areas in subbasin # 2 in 2019 compared to 2001 (Figure 33). The increase in mean monthly streamflow using the 2019 land use increased by 5% to 35% in subbasin #2 (Figure 34), and percentage flow changes across the subbasin ranged from 0.5 to 50% (Figure 35).

Figure 33. Land use in 2001 and 2019

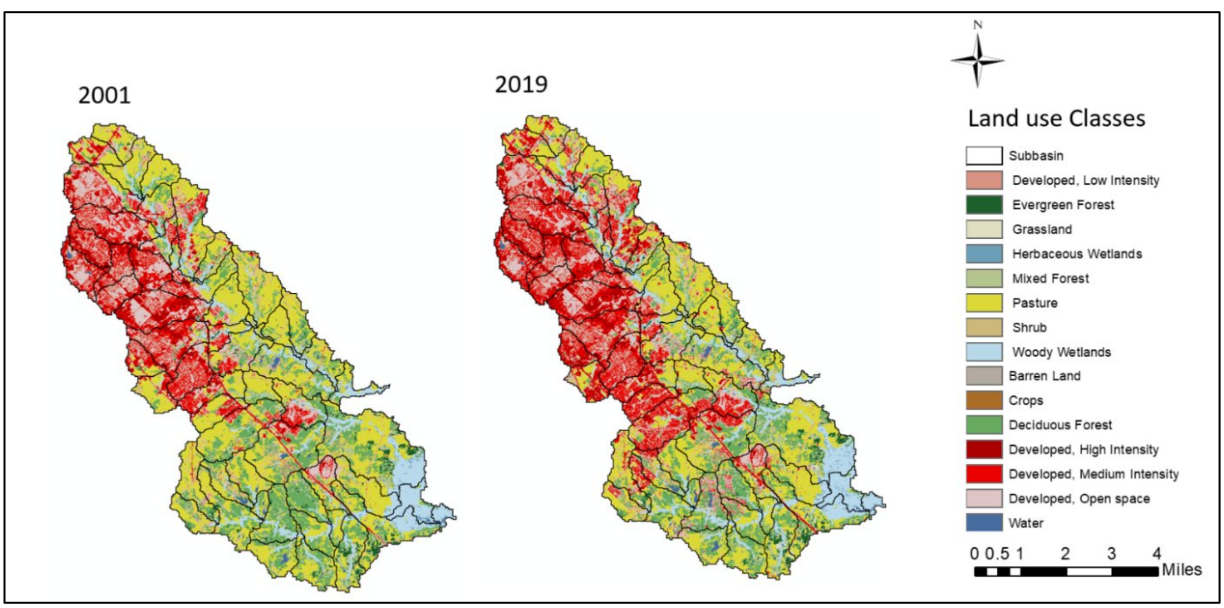

Figure 34. Percentage change in mean monthly flow for land use of 2001 and 2019 for subbasin 2.

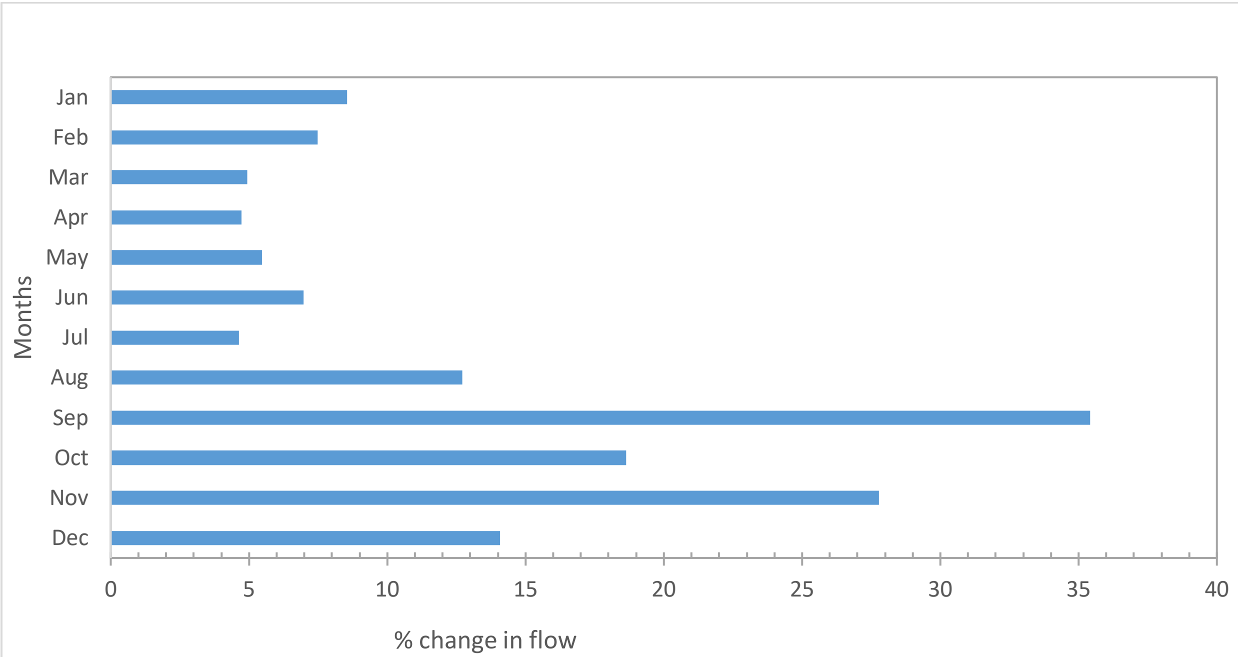

Figure 35. Percentage flow changes across the watershed (subbasins)

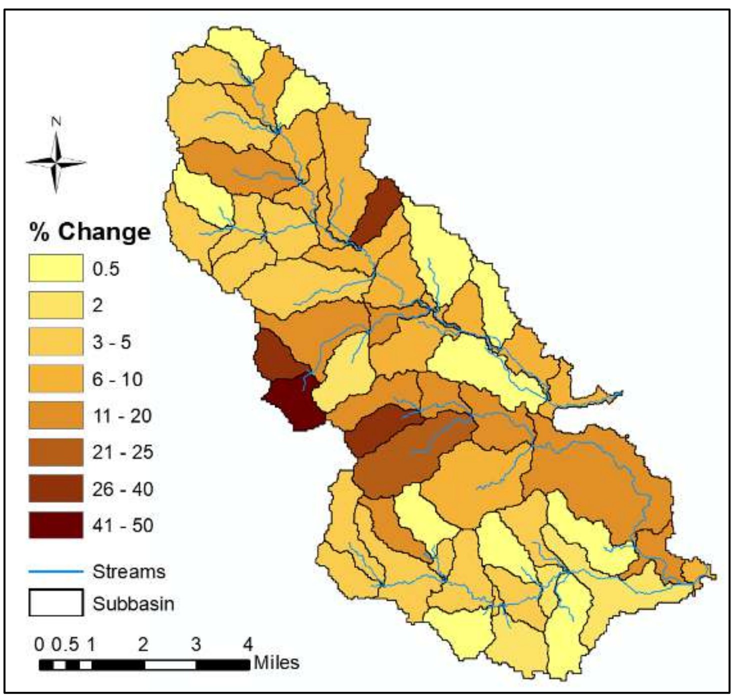

Effect of Precipitation Magnitude Change

This scenario is based on changes in magnitude and frequency of extreme precipitation. Precipitation event of May 11-20, 2015 was increased by 20% across the entire watershed. Results of this simulation were compared to those of simulation with the original precipitation of the same events. Simulated flows of the two scenarios were compared. These results show that the 20% increase in precipitation resulted in 8% and 32% increase of the first and second stream flow peaks compared to stream flow generated by the original precipitation (Figure 36).

Figure 36. The effect of precipitation magnitude changes on discharge near Bryan, TX

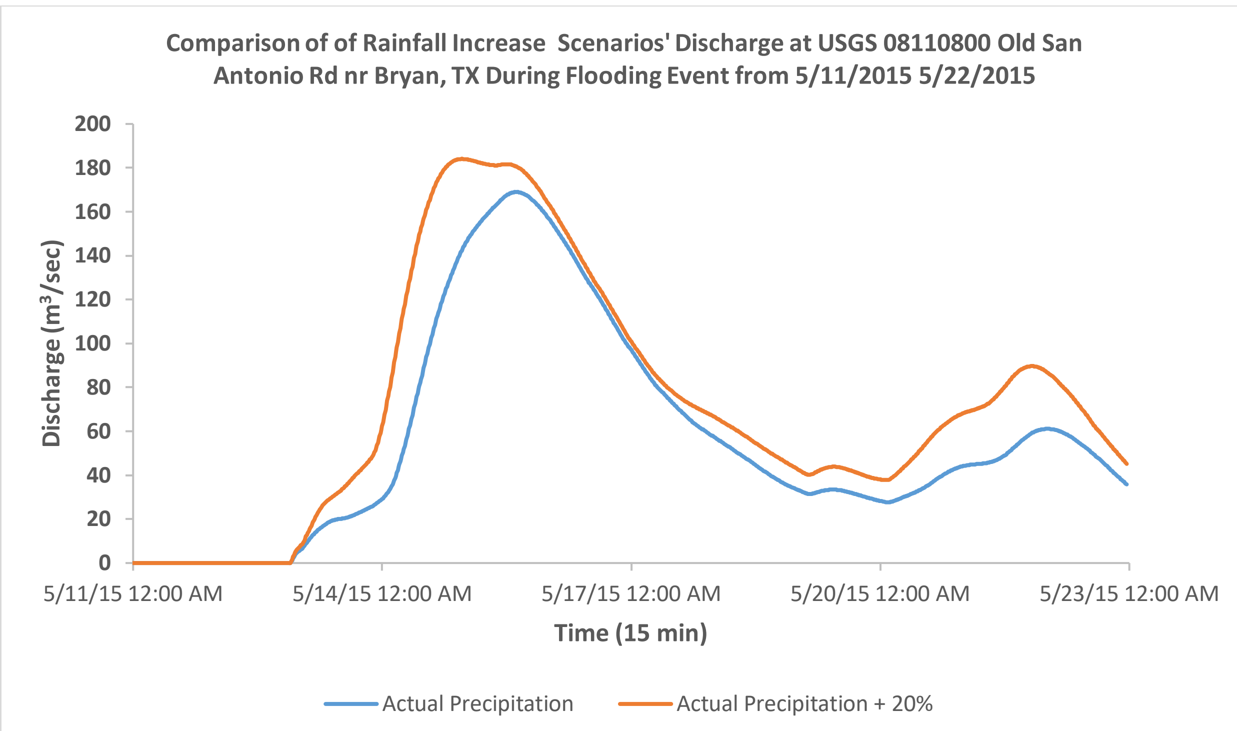

We also used the SWAT model to analyze the impact of the increase in precipitation on streamflow by increasing the watershed precipitation by 20% across the watershed. Number of flood events were grouped in three categories: minor (=> 3500 CFS), moderate (=> 11600 CFS), and major (=> 37000) floods for actual precipitation and actual precipitation + 20%. The 20% increase in precipitation resulted in a 200% increase in the major floods (Figure 37).

Figure 37. Flood frequencies of minor (=> 3500 CFS), moderate (=> 11600 CFS), and major (=> 37000) floods for actual and 20% increased precipitation (2005-2020)

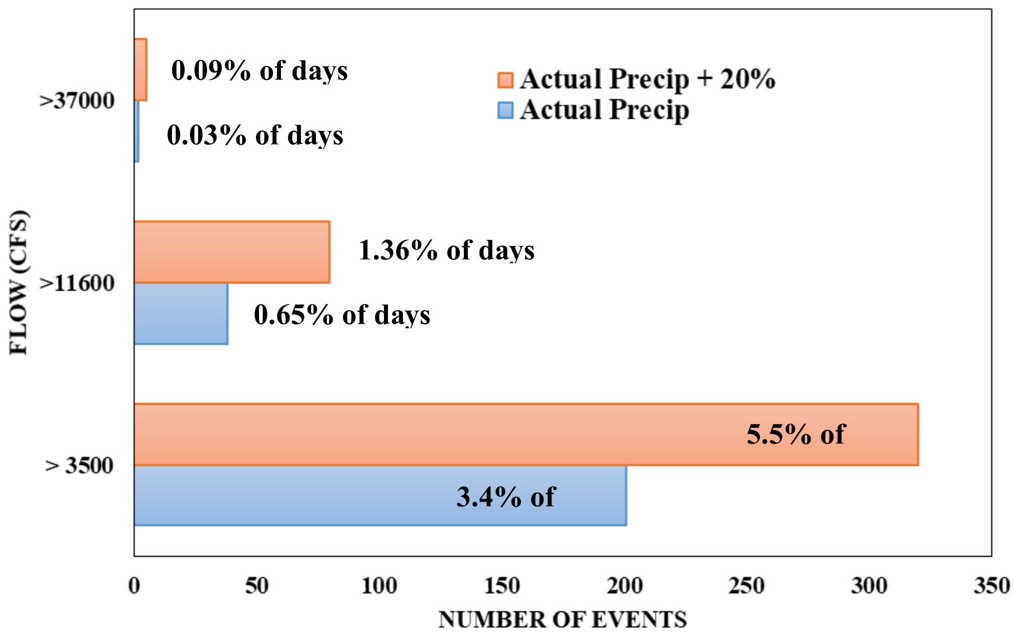

References:

Downner, C.W.; Ogden, F.L., 2004. GSSHA: Model to simulate diverse stream flow producing processes. *J. Hydrol. Eng*., 9, 161–174.

Pettitt, A.N., 1979. A non-parametric approach to the change-point problem. J. R. Statist. Soc. Series C (Applied Statistics) 28, 126–135. https://doi.org/10.2307/2346729.

Kendall, M.G., 1970. Rank Correlation Methods (4th ed). Griffin and Co. Ltd.

Kendall, M., Stuart, A., Ord, K.J., Arnold, S., 1999. Kendall's Advanced Theory of Statistics: Volume 2A-Classical Inference and the Linear Model (Kendall's Library of Statistics). A Hodder Arnold Publication

Kisi, O., Ay, M., 2014. Comparison of Mann-Kendall and innovative trend method for water quality parameters of the Kizilirmak River. Turkey. *J. Hydrol.* 513 (5), 362–375